Date of publication Dec. 25, 2020, date of current version Dec. 25, 2020.

Digital Object Identifier 10.46470/03d8ffbd.b48be62a

Multiple MIMO with Joint Block Antenna Number Modulation and Adaptive Antenna Selection for Future Wireless Systems

MUHAMMET KIRIK[1], JEHAD M. HAMAMREH[1]

[1]M. Kirik and J. M. Hamamreh are with WISLAB-TELENG for Wireless Research at the Department of Electrical-Electronics Engineering, Antalya Bilim University, Antalya, Turkey. (web: https://sites.google.com/view/wislab // email: muhammet.kirik@std.antalya.edu.tr).

Corresponding author: Muhammet Kirik (e-mail: muhammet.kirik@std.antalya.edu.tr).

The Matlab simulation codes used to generate the results in this paper can be found at https://researcherstore.com with the name M-MIMO-ANM. This research was partly funded by TUBITAK under Grant/Award Number 119E392.

ABSTRACT Multiple MIMO with joint block Antenna Number Modulation (M-MIMO-ANM) is proposed in this paper as a novel transmission method that exploits the features of both Massive Multiple Input Multiple Output (M-MIMO) and Antenna Number Modulation (ANM) concepts. In this scheme, the main purpose is to increase the number of additionally transmitted data bits, which are sent without any consumption in the bandwidth. To achieve this, the antenna elements of a large array are divided into blocks, whose numbers are utilized to convey additional data bits along with those bits sent by the number of antenna elements within each block as well as those sent by conventional modulation schemes (e.g., BPSK). The implementation of M-MIMO-ANM scheme relies on the idea of dividing the whole antenna array into blocks, where each block corresponds to a group of bits depending on the total number of available blocks, thus ANM concept is applied not only to the antennas within each block but also to the blocks forming the entire antenna array. This creates an opportunity to convey even more additional data bits, compared with the conventional ANM scheme, while there is a noticeable improvement in the reliability of data transmission. With all these dynamics, M-MIMO-ANM concept is a candidate to create a new perspective to the Internet of Things (IoT) applications, with its energy efficient, spectrum efficient, robust, and both data and channel dependent data transmission nature that comes from the properties of Massive MIMO and ANM. The introduced system is investigated, and its validity is proven, where analytical and simulation results in terms of the bit error rate (BER) and throughput of the system are given. The numerical computer simulations furthermore compare the performances of M-MIMO-ANM with MIMO-ANM to show its superiority, and the advantages of the concept are discussed. M-MIMO-ANM is promising a highly reliable and resilient system thanks to its cascaded simultaneous bit transmission by the different number of antenna blocks and antenna elements within each block.

INDEX TERMS MIMO, M-MIMO-ANM, block number modulation, antenna number modulation, adaptive antenna selection, spatial modulation, Rayleigh Channel, BER, Wireless Communication, 6G.

I. INTRODUCTION

THE increasing demand for high speed, high spectral efficiency, high reliability, and low power consumption in online Internet devices, which have emerged due to the recent developments and unprecedented advances in communication and computation technologies, is pushing researchers to develop advanced and more effective transmission methods and techniques such as Massive MIMO that includes all the benefits of conventional MIMO, but doing this by using a large number of antennas at the base stations (BSs) to harvest more performance advantages [1]–[4].

As a promising technique in the applications of 5G, Massive MIMO obtains a solid place with its simultaneous multi-user servicing nature, in wireless standards like 5G, and LTE [5], [6]. In addition to multi-user service, Massive MIMO also exhibits superior performance in spectral efficiency over

the standards established on a small number of antennas [7], [8]. Aside from spectral efficiency, Massive MIMO is also capable of providing better channel reliability due to its diversity gain along with having low propagation loss [9]. In spite of all these advantages [10], which promote Massive MIMO to be an adopted technology in 5G wireless systems in a centralized or decentralized setup [11], [12], there are still some certain issues that Massive MIMO suffers from, such as the hardware and signal processing costs that increase as the number of antenna elements in BSs increases [13].

The second issue is the RF chain complexity that inevitably comes with the dedication of RF chains for each antenna element [14], especially for Massive MIMO systems that contain roughly 50-400 antennas in each BS to serve multiple antenna users at the same time [15]. Another issue is the inter-channel interference (ICI) that occurs because of the overlapping of the signals that are emitted from the vast number of antennas [16].

To overcome these issues, an effective antenna selection algorithm could be a wise solution to reduce the number of RF chains by choosing the antennas that offer the highest signal rate [17], [18], which enables the system to convey the data bits with much less channel effect, and consequently much less cost, complexity, and ICI, while the system performance is not sacrificed. In this regard, several antenna selection methods have been offered throughout the years. One of these methods mentioned in [18] relies on the idea that suggests choosing the antennas that have the maximum channel capacity under a perfect channel state information (CSI) assumption as a selection criteria. One other worthy to mention idea is based on solving the maximum volume offering submatrix in the whole antenna matrix instead of solving it directly as an antenna selection method, which is deeply investigated in [19]–[21]. In addition to these aforementioned antenna selection techniques, several variations of MIMO schemes have been adapted to Massive MIMO literature, such as [3], [22], to offer a remedy for the cost, channel complexity and ICI issues of Massive MIMO. However, all these offered antenna selection methods created for the usage of Massive MIMO systems within the adaptations of MIMO schemes that are inherited from spatial modulation (SM), both have the same sufferings, that is the inability to make the antenna selections both channel and data dependent at the same time [23]–[25].

On the other hand, a recent study called Antenna Number Modulation (ANM) [26], which is applied to MIMO systems opens the door to create a possibility to make the antenna selection to be both data and channel dependent at the same time thanks to its nature that allows the additional data bits to be sent by the number (not indices) of active antennas in the system. Within this scheme, a portion of the incoming data stream is separated to determine the active antenna numbers in the system to convey the rest of the data stream by using conventional PSK/QAM modulation.

In an effort to further improve the data rate and reliability performance of the recently proposed MIMO-ANM scheme, in this paper, a novel method called Multiple Multiple Input Multiple Output with joint block Antenna Number Modulation (M-MIMO-ANM) is proposed for combining the benefits of both of the above mentioned schemes Massive MIMO and ANM. In this method, the antenna elements of a relatively large scale antenna array are grouped at the Base Station (BS) into blocks, whose number is used as an additional feature that can convey extra information bits. This is done by assigning a portion of the data stream for the number of antenna blocks and assigning another portion of data stream for the transmit antennas within each active block, whereas the remaining part of the data stream is sent by using conventional PSK/QAM modulation. The aim of the second part of this research is to improve the performance of the aforementioned scheme by proposing and designing a novel transmission M-MIMO-ANM scheme that can make the selection of the antenna blocks and transmit antennas in each antenna block to be both channel and data dependent simultaneously in a large scale of antenna system. To sum up, the proposed Multiple MIMO-ANM scheme is a promising technique, in terms of spectral efficiency, enhanced reliability, low complexity, and secrecy that comes from the inherits of Massive MIMO and ANM.

The following parts of this paper are organized as follows. In section II, system model of the Multiple MIMO-ANM is explained, details of the concept are analyzed with mathematical equations, and comprehensive illustrations; and a sample scenario is exemplified. In section III, the adaptive antenna selection ability of Multiple MIMO-ANM system is interrogated, the applicability of the system is analyzed by mathematical equations, and the understanding of the process is strengthened by an example. In section IV, performance analysis of the scheme is discussed. In section V, simulation results of regarding scheme and its comparisons with other schemes are shown. Lastly, section VI concludes the paper.

II. SYSTEM MODEL

In this paper, a single user MIMO scheme under Rayleigh channel is considered. The number of blocks and number of transmit antennas are notated as B and T respectively while the number of receive antennas is notated as R. For simplicity, number of receiver antennas is kept singular, $i.e.$ $R = 1$.

This introduced novel transmission method, called M-MIMO-ANM, manipulates both the number of antenna blocks and the number of antennas that are situated in these blocks to send even more data bits per antenna than conventional MIMO-ANM scheme [26]. This creates a new dimension, called number of blocks in addition to dimensions that come from PSK/QAM and the number of antennas in space domain.

This results in a 4D modulated scheme that exploits the number of antenna array blocks, in addition to in-phase, quadrature components of the signal constellation diagram, and number of antennas that is already proposed in conventional MIMO-ANM.

A. THE TRANSMISSION STRUCTURE OF M-MIMO-ANM

The general structure of the proposed M-MIMO-ANM transmitter is shown in Fig. 1.

In the given data stream, symbols are separated into three sub-streams. The first sub-stream is named as the "Main Bits", and the symbols in this sub-stream are the actual symbols intended to be sent. The second sub-stream is named as the "BNM Bits", and the symbols in this sub-stream define how many antenna blocks will be used in the antenna system. The third sub-stream is named as the "ANM Bits", and the symbols in this data stream define how many antennas in each block will be deployed. By doing this separation, each individual element of the Main Bits sub-stream can be sent according to the BNM Bits and the ANM Bits sub-streams.

After this stage that is achieved by separating the total number of bits $N = N_1 + N_2 + N_3$ into the "Main Bits" (N_1), which is determined by the signal constellation modulation order (BPSK, QPSK, QAM, etc.) M calculated by the formula of $N_1 = \log_2(M)$, "BNM Bits" (N_2), which is determined by the number of active antenna blocks at the transmission side B calculated by the formula of $N_2 = \log_2(B)$, and the "ANM Bits" (N_3), which is determined by the number of available transmit antennas in each active block T calculated by the formula of $N_3 = \log_2(T)$, the Main Bits are modulated by one of those conventional BPSK, QPSK, or different variations of QAM, while the BNM Bits are utilized to modulate the number of blocks by creating a look-up table that maps BNM Bits' groups into a specific number of active blocks to make the decision to define how many antenna blocks will be activated. In a similar way, the ANM Bits are utilized to modulate the number of antennas by creating a look-up table that maps ANM Bits' groups into a specific number of active antennas to make the decision to define how many antenna elements in each block will be activated.

As a predefined case, where the total number of antenna blocks in the system is four and the total number of antenna elements in each block is four ($i.e., B = 4, T = 4$), the mapping tables are shown for BNM Bits and ANM Bits in Table I and Table II, respectively.

TABLE 1: BNM mapper with N_2=2 bits & B=4

BNM bits (N_2)	Active Antenna Blocks Pattern (ζ)
[0 0]	[1; 0; 0; 0]
[0 1]	[1; 1; 0; 0]
[1 0]	[1; 1; 1; 0]
[1 1]	[1; 1; 1; 1]

TABLE 2: ANM mapper with N_3=2 bits & T=4

ANM bits (N_3)	Active Antennas Pattern ($\mathbf{v}$)
[0 0]	[1; 0; 0; 0]
[0 1]	[1; 1; 0; 0]
[1 0]	[1; 1; 1; 0]
[1 1]	[1; 1; 1; 1]

To have a more clear aspect in Table I, if the BNM Bits group or couple is "00" this means the number of active blocks is one, if it is "01" this means the number of active blocks is two, if it is "10" this means the number of active blocks is three, and if it is "11" this means the number of active blocks is four. The mapping numbers of each block is defined by the number of antenna blocks in the system. A similar explanation to clarify the process in Table II can also be expressed for ANM Bits as follows. If the ANM Bits group or couple is "00" this means the number of active antennas in a block is one, if it is "01" this means the number of active antennas in a block is two, if it is "10" this means the number of active antennas in a block is three, and if it is "11" this means the number of active antennas in a block is four. The mapping numbers of each antenna is defined by the number of antennas in the system. If $B = 2^{N_2}$ is assumed as the number of the transmit antenna blocks and $T = 2^{N_3}$ is assumed as the number of the transmit antennas in each block in the system, where N_2 represents the number of data bits for each BNM Bits group and N_3 represents the number of data bits for each ANM Bits group. For example, for four antenna blocks and eight antenna elements in each block $B = 2^{N_2} = 4$, $N_2 = \log_2(B) = 2$ and $T = 2^{N_3} = 8$, $N_3 = \log_2(T) = 3$, then the BNM Bits grouping possibilities are in two bits as $00, 01, 10, 11$, whereas the total possibilities for ANM Bits are grouped in three bits from 000 till 111. To acquire the most optimized results in this scheme and simplify its demonstration, the case is established on four transmit antenna blocks ($B = 4$), four transmit antenna elements in each block ($T = 4$), and one receive antenna ($R = 1$).

As the next step of modulating "Main Bits" with respect to different varieties of signal modulation constellation types (i.e., BPSK, QPSK, 16QAM, 64QAM), "BNM Bits", and "ANM Bits", each individual formed data symbol (x) is conveyed from the active antennas, which are specifically activated according to their positions in certain antenna block. This specific antenna activation is operated according to Table I and Table II. After that, the transmitted data symbol is multiplied by the flat fading coefficients of the blocks, which are obtained by the average value of each four antennas that are adjacent to each other, and also multiplied by the active antennas in each active antenna group. The acquired result is then summed by the noise (w) with zero mean and N_0 variance at the receive antenna to acquire the signal that reaches the receiver. As a result, the formula of 1×16 MISO system model for each symbol in this scheme is given as

$$y = \sqrt{\frac{P}{Z \times V}} \times \mathbf{g} \times \zeta \times \mathbf{h} \times \mathbf{v}_e \times x + w, \qquad (1)$$

where P is the power required for the transmission of each data symbol x, $Z = \|\zeta\|_2 = \sum_{i=1}^{B} \zeta_i^2$ is the total number of active blocks in the entire antenna array, and $V = \|\mathbf{v}\|_2 = \sum_{i=1}^{T} v_i^2$ is the total number of active antennas in each active block. $\mathbf{v}_e = [\mathbf{v}; \mathbf{v}; \mathbf{v}; \mathbf{v}] \in \mathbb{B}^{16\times 1}$ is the activation vector of all the antenna array elements of the

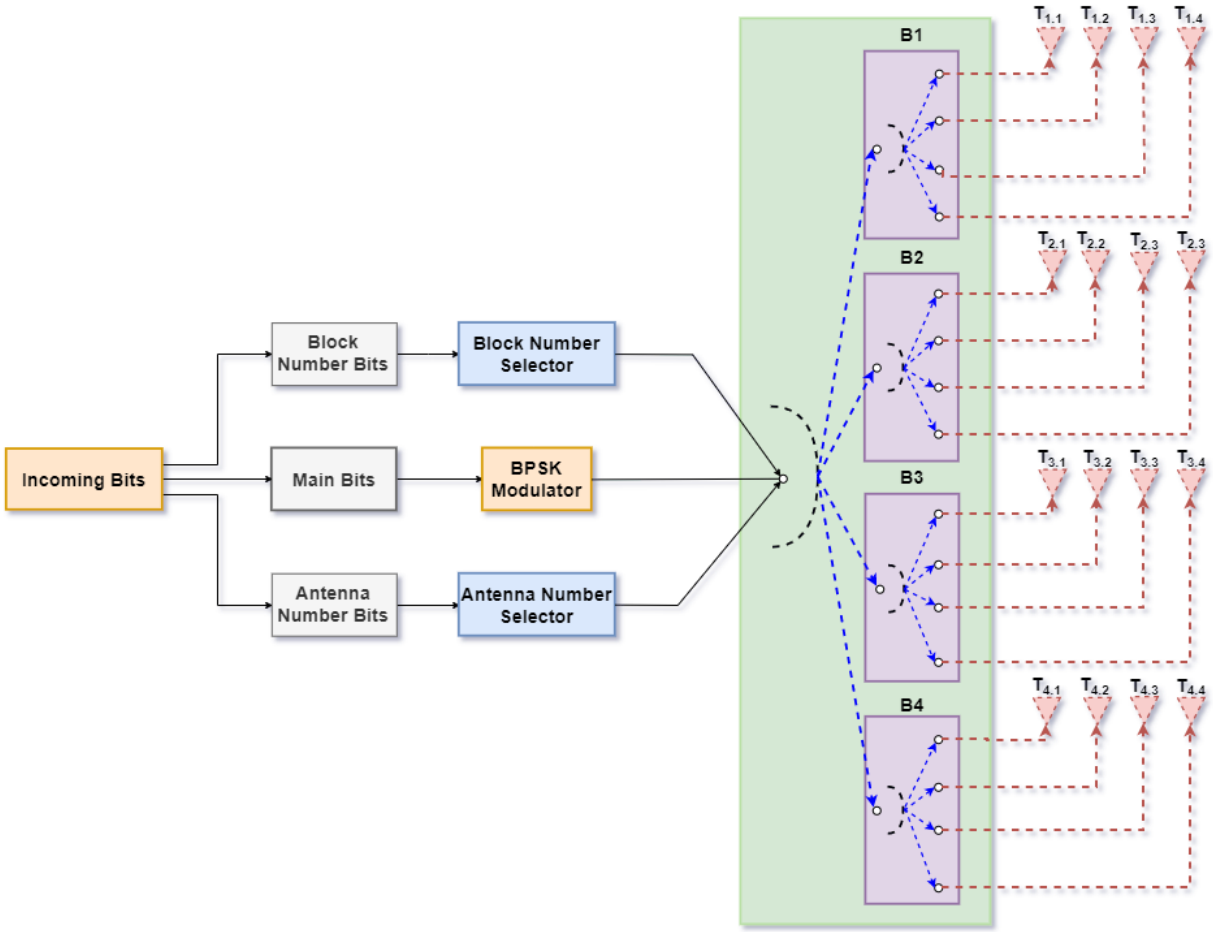

FIGURE 1: Transmitter structure of M-MIMO-ANM.

system, in which $\mathbf{v} = [v_1; v_2; v_3; v_4] \in \mathbb{B}^{4\times 1}$ is the activation pattern vector corresponding to a single block, whose elements are Boolean ($\mathbb{B}$), i.e., zero or one. In addition to that, $\mathbf{h} = [h_{11}, h_{12}, h_{13}, h_{14}, h_{15}, h_{16}, h_{17}, h_{18}, h_{19}, h_{110}, h_{111}, h_{112}, h_{113}, h_{114}, h_{115}, h_{116}] \in \mathbb{C}^{1\times 16}$ is the flat fading channel vector, in which h_{RT} represents a Gaussian channel coefficient with zero mean and unity variance that corresponds to the connection between the $T'th$ transmit antenna, which is situated in $B'th$ antenna block, and $R'th$ receive antenna. $\mathbf{g} = [g_1, g_2, g_3, g_4] \in \mathbb{C}^{1\times 4}$ is the artificially[1] introduced flat fading channel vector for the antenna blocks in the system, which is acquired by the average values of each four $\mathbf{h}$ values that are adjacent to each other as shown below: $g_1 = \frac{h_{11}+h_{12}+h_{13}+h_{14}}{4}$, $g_2 = \frac{h_{15}+h_{16}+h_{17}+h_{18}}{4}$, $g_3 = \frac{h_{19}+h_{110}+h_{111}+h_{112}}{4}$, $g_4 = \frac{h_{113}+h_{114}+h_{115}+h_{116}}{4}$, $\zeta \in \mathbb{B}^{4\times 1}$ is the activation pattern vector that is created to determine the inactive antenna blocks by zeros and the active antenna blocks by ones according to N_2 bits and mapping process indicated in Table I, whereas $\mathbf{v} \in \mathbb{R}^{4\times 1}$ is the activation pattern vector that is created to determine the inactive antennas in each active antenna block by zeros and active antennas in each active antenna block by ones according to N_3 bits and mapping process indicated in Table II. [2]

In addition to the antenna number feature of the MIMO system, the capability of M-MIMO-ANM is offering even more spectral and power efficiency with its block number feature. Moreover, by conserving the nature of MIMO-ANM's independent mapping process of the indices or position of the antennas, the simultaneous channel and data dependency sustains the advantage that the spatial index modulation cannot offer [27], [28], as shown in the following example.

Example: To clarify the process and improve the understanding of the concept a comprehensive example is submitted as follows. Assume a small sample of data bit sequence that is given as "101101101011011", and this data stream is desired to be sent by a $B \times T \times R = 4 \times 4 \times 1$ M-

[1]It is intentionally introduced to the system to help the receiver in the detection process of the number of active blocks.

[2]The g values for this case are set as the average values of the channel coefficients to create a pattern in the activation of the antenna blocks from the highest quality offering to lowest, without disrupting the credibility of the system while the antenna selection algorithm is applied. The various number of throughput acquired from the simulation results prove that the most robust method to deploy the antenna blocks in M-MIMO-ANM is setting the g values as not any arbitrary number but an h dependent variable.

MIMO-ANM system using BPSK modulation, which also can be considered as $T_{Total} \times R = 16 \times 1$. Since there are four antenna blocks in the given system, determination of the number of different BNM group is operated by the previously given formula $2^{N_2} = B = 4$. With this formula, the number of bits in each BNM group can be found as $N_2 = \log_2 B = 2$. To find N_3, the number of bits in each ANM subgroup, a similar formula $2^{N_3} = T = 4$, which is also previously given leads that $N_3 = \log_2 T = 2$. These results, $N_2 = 2, N_3 = 2$, imply that for the transmission of each element of the Main Bits group that is modulated by BPSK, there are two bits in the BNM Bits group that activate the antenna blocks, and there are two bits in the ANM Bits group that are assigned to activate the transmit antennas in each block according to their bit numbers. This separation of the incoming data bits as Main Bits (modulated by BPSK), BNM Bits (modulated by the number of antenna blocks), ANM bits (modulated by the number of antennas in each block) for this example is shown in Fig.2.

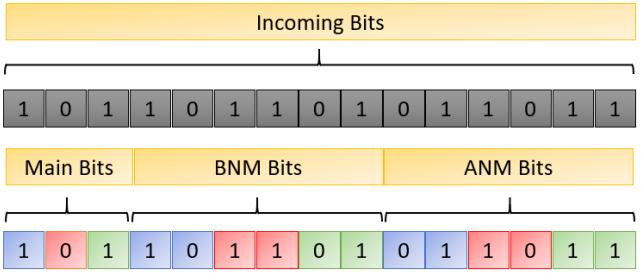

FIGURE 2: Main Bits, BNM Bits and ANM Bits Separation from Incoming Data Stream for 4 Antenna Blocks, 4 Transmit Antennas and 1 Receiver Antenna when BPSK is used.

After the bit separation, M-MIMO-ANM process proceeds as follows. To send the first element of the Main Bits group, first two bits of the BNM Bits group and first two bits of the ANM Bits group are taken under consideration. As it is seen in Fig.2, these correlated bits are indicated by blue color. According to these bits, it can be inferred that the transmission of 1 is operated by three blocks, since the 10 in the BNM Bits group corresponds to three blocks, and two transmit antennas that are situated in these three blocks activated, since the 01 refers to two antennas in each active block. The transmission of the second bit of the Main Bits group is executed by the second pairs of both BNM Bits and ANM Bits group, which are colored by red in Fig. 2 Within these bits, it can be stated that 0 is conveyed by three antennas that are located in each of the four antenna block in the system, since the 11 in the BNM Bits group means the activation of four antenna blocks, and 10 in the ANM Bits group means the activation of three antennas in each activated block. Lastly, the third element of the main bits group is conveyed by the third pairs of the BNM Bits group and ANM Bits group, which are specified by green color. According to these pairs, the transmission of 1 is achieved by two blocks, since the 01 in the BNM Bits block regards to two antenna blocks, and each of these two antenna blocks contains four active transmit antennas, since the 11 in the ANM Bits group means activation of two antennas in each active antenna block. The visualized scheme of this process is displayed in Fig. 3.

Since there are different possibilities to convey the main signals from different blocks and antennas, the corresponding received main signal may vary according to those blocks and antennas in usage. These variations for received main signal expressions are listed in the following equations.

When active blocks' number is one and active antennas' number in each active block is one, the received signal is given as

$$y_1 = \sqrt{\frac{P}{1 \times 1}} \times (g_1) \times (h_{11}) \times x_i + w. \tag{2}$$

When active blocks' number is one and active antennas' number in each active block is two, the received signal is given as

$$y_2 = \sqrt{\frac{P}{1 \times 2}} \times (g_1) \times (h_{11} + h_{12}) \times x_i + w. \tag{3}$$

When active blocks' number is one and active antennas' number in each active block is three, the received signal is given as

$$y_3 = \sqrt{\frac{P}{1 \times 3}} \times (g_1) \times (h_{11} + h_{12} + h_{13}) x_i + w. \tag{4}$$

When active blocks' number is one and active antennas' number in each active block is four, the received signal is given as

$$y_4 = \sqrt{\frac{P}{1 \times 4}} \times (g_1) \times (h_{11} + h_{12} + h_{13} + h_{14}) x_i + w. \tag{5}$$

When active blocks' number is two and active antennas' number in each active block is one, the received signal is given as

$$y_5 = \sqrt{\frac{P}{2 \times 1}} \times [(g_1) \times (h_{11}) + (g_2) \times (h_{15})] x_i + w. \tag{6}$$

When active blocks' number is two and active antennas' number in each active block is two, the received signal is given as

$$y_6 = \sqrt{\frac{P}{2 \times 2}} \times [(g_1) \times (h_{11} + h_{12}) + (g_2) \times (h_{15} + h_{16})] x_i + w. \tag{7}$$

When active blocks' number is two and active antennas' number in each active block is three, the received signal is given as

$$y_7 = \sqrt{\frac{P}{2 \times 3}} \times [(g_1) \times (h_{11} + h_{12} + h_{13}) + (g_2) \times (h_{15} + h_{16} + h_{17})] x_i + w. \tag{8}$$

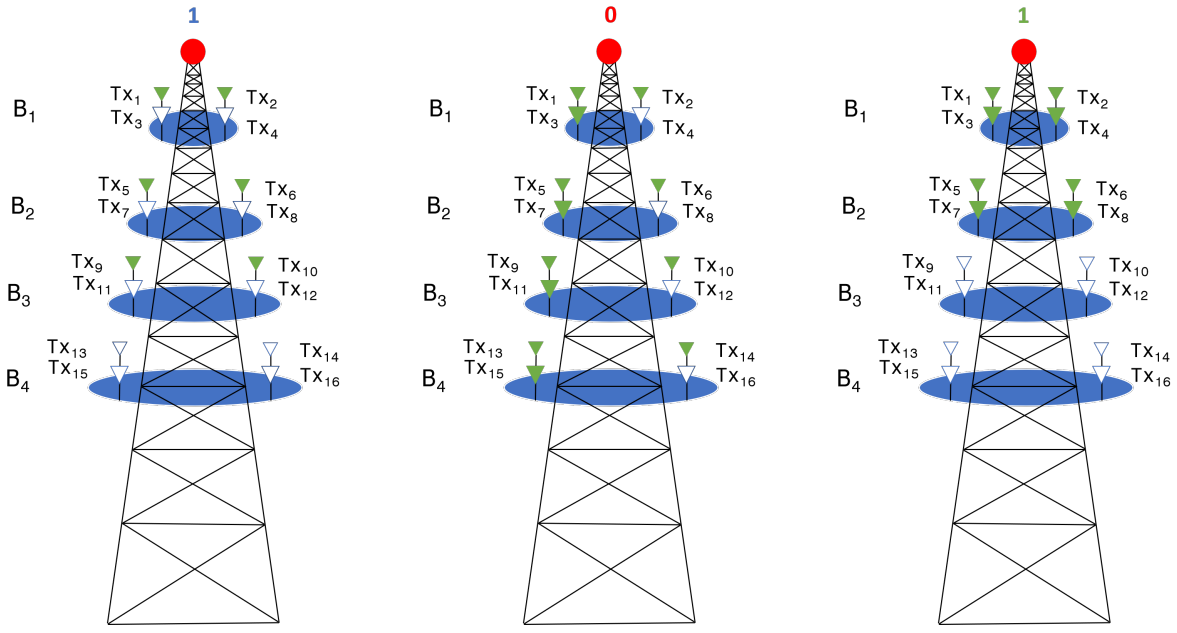

((a)) Transmission of 1 via three blocks two antennas in each block.

((b)) Transmission of 0 via four blocks three antennas in each block.

((c)) Transmission of 1 via two blocks four antennas in each block.

FIGURE 3: Simple visualization of the antenna activation process and mapping in M-MIMO-ANM scheme.

When active blocks' number is two and active antennas' number in each active block is four, the received signal is given as

$$y_8 = \sqrt{\frac{P}{2\times 4}} \times [(g_1) \times (h_{11} + h_{12} + h_{13} + h_{14}) + (g_2) \times (h_{15} + h_{16} + h_{17} + h_{18})]x_i + w. \quad (9)$$

When active blocks' number is three and active antennas' number in each active block is one, the received signal is given as

$$y_9 = \sqrt{\frac{P}{3\times 1}} \times [(g_1) \times (h_{11}) + (g_2) \times (h_{15}) + (g_3) \times (h_{19})]x_i + w \quad (10)$$

When active blocks' number is three and active antennas' number in each active block is two, the received signal is given as

$$y_{10} = \sqrt{\frac{P}{3\times 2}} \times [(g_1) \times (h_{11} + h_{12}) + (g_2) \times (h_{15} + h_{16}) + (g_3) \times (h_{19} + h_{110})]x_i + w \quad (11)$$

When active blocks' number is three and active antennas' number in each active block is three, the received signal is given as

$$y_{11} = \sqrt{\frac{P}{3\times 3}} \times [(g_1) \times (h_{11} + h_{12} + h_{13}) + (g_2) \times (h_{15} + h_{16} + h_{17}) + (g_3) \times (h_{19} + h_{110} + h_{111})]x_i + w \quad (12)$$

When active blocks' number is three and active antennas' number in each active block is four, the received signal is given as

$$y_{12} = \sqrt{\frac{P}{3\times 4}} \times [(g_1) \times (h_{11} + h_{12} + h_{13} + h_{14}) + (g_2) \times (h_{15} + h_{16} + h_{17} + h_{18}) + (g_3) \times (h_{19} + h_{110} + + h_{111} + h_{112})]x_i + w \quad (13)$$

When active blocks' number is four and active antennas' number in each active block is one, the received signal is given as

$$y_{13} = \sqrt{\frac{P}{4\times 1}} \times [(g_1) \times (h_{11}) + (g_2) \times (h_{15}) + (g_3) \times (h_{19}) + (g_4) \times (h_{113})]x_i + w \quad (14)$$

When active blocks' number is four and active antennas' number in each active block is two, the received signal is given as

$$y_{14} = \sqrt{\frac{P}{4\times 2}} \times [(g_1) \times (h_{11} + h_{12}) + (g_2) \times (h_{15} + h_{16}) + (g_3) \times (h_{19} + h_{110}) + (g_4) \times (h_{113} + h_{114})]x_i + w \quad (15)$$

When active blocks' number is four and active antennas' number in each active block is three, the received signal is

given as

$$y_{15} = \sqrt{\frac{P}{4 \times 3}} \times [(g_1) \times (h_{11} + h_{12} + h_{13}) + (g_2) \times (h_{15} + h_{16} + h_{17}) + (g_3) \times (h_{19} + h_{110} + h_{111}) + (g_4) \times (h_{113} + h_{114} + + h_{115})]x_i + w \quad (16)$$

When active blocks' number is four and active antennas' number in each active block is four, the received signal is given as

$$y_{16} = \sqrt{\frac{P}{4 \times 4}} \times [(g_1) \times (h_{11} + h_{12} + h_{13} + h_{14}) + (g_2) \times (h_{15} + h_{16} + h_{17} + h_{18}) + (g_3) \times (h_{19} + h_{110} + h_{111} + h_{112}) + (g_4) \times (h_{113} + h_{114} + + h_{115} + h_{116})]x_i + w \quad (17)$$

B. THE RECEPTION STRUCTURE OF M-MIMO-ANM

The corresponding reception side structure of M-MIMO-ANM is given in Fig. 4.

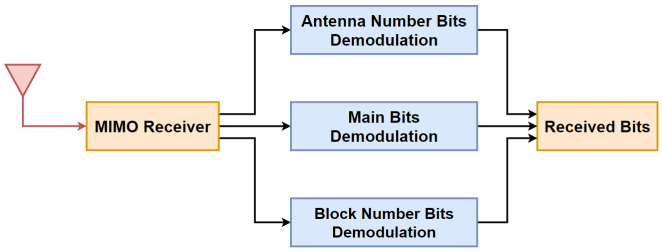

FIGURE 4: Receiver Structure of M-MIMO-ANM.

To detect the data bits that come from both conventional M-ary signal constellation symbols, the number of antenna blocks and the number of antennas in each block at the receiver side, different approaches of detection methods can be used. One of these approaches is joint detection of Main Bits, BNM Bits, ANM Bits, whereas the other approach is individual detections independently separate from each other in a successive manner. Further explanation about these two methods is provided below.

Demodulation of the data bits can be operated under a common detection process for both Main Bits, which is modulated by either one of those BPSK, QPSK, 16QAM, or 64QAM, BNM Bits, and ANM Bits, or a sequential detection can be applied individually by demodulating the BNM Bits first, then demodulating ANM Bits, then demodulating Main Bits with respect to demodulations of BNM Bits and ANM Bits. It should be stated that by applying a common detection procedure at the reception side, the complexity of the system is dramatically increased. The reason behind that is, by applying a joint detection, the number of operations becomes $B \times T \times M$, while in the separated detection this number is $B + T + M$.

In the joint demodulation of Main Bits, BNM Bits, and ANM Bits, a Maximum Likelihood (ML) detector can be used to detect the active blocks, active antennas in these active blocks, and signal constellation points at once. The regarded formula for this detector can be derived as

$$J_{\zeta,v,x} = \min_{\hat{x},\hat{\zeta},\hat{v}} \left(||y - \left(\sum_{i=1}^{\hat{\zeta}} g_i \right) \left(\sum_{i=1}^{\hat{v}} h_{1i} \right) \hat{x}||^2 \right), \quad (18)$$

where $\zeta \in 1, 2, 3, 4$ is the possible number of active antenna blocks, $v \in 1, 2, ..., 16$ is the possible number of active antennas in the system, $y_i \in y_1, y_2, ..., y_{16}$ is the received signals that is defined by certain combinations of active antenna blocks and antennas in these active blocks, and x_i is the estimated constellation symbols.

On the other hand, the individual detection of the Main Bits, BNM Bits, and ANM Bits, that provides less complexity might be a wiser alternative in some certain cases that requires low delay, less processing, and less power consumption, like IoT devices. In such a case, the ML detector formulas for each individual group of bits as BNM Bits, ANM Bits, Main Bits are given as

$$J_\zeta = \min_{\hat{\zeta}} \left(||y - \left(\sum_{i=1}^{\hat{\zeta}} g_i \right) x||^2 \right), \quad (19)$$

$$J_v = \min_{\hat{v}} \left(||y - \left(\sum_{i=1}^{\hat{v}} h_{1i} \right) x||^2 \right), \quad (20)$$

$$J_x = \min_{\hat{x}} \left(||y - \left(\sum_{i=1}^{v} h_{1i} \right) \hat{x}||^2 \right). \quad (21)$$

As it can be seen from (21), the g values which were set as the average values of the channel coefficients in each corresponding block do not have an effect at the reception side of M-MIMO-ANM. The reason why behind that is, the g is used only for creating an activation pattern for the antenna blocks. Since the deployment of the g values in (21) would create an artificial performance increment and obstruct to reflect the true performance of the system, it is not considered as a parameter of the detection of Main Bits.

During the simulation process of this scheme, detection of the bits are achieved individually due to its aforementioned advantages.

III. MULTIPLE MIMO WITH JOINT BLOCK ANTENNA NUMBER MODULATION AND ADAPTIVE ANTENNA SELECTION (M-MIMO-ANM-AAS)

In this section, the main advantage of the MIMO-ANM system over MIMO-SM, which is the ability to make antenna selection channel dependent as well as data dependent is offered as an improved version of Multiple Input Multiple Output System with Antenna Number Modulation and Adaptive Antenna Selection (MIMO-ANM-AAS). The source of this improvement relies on making the antenna selection not only based on channel coefficients of each individual antenna, but considering each antenna in each block as a member of a team and acquiring the total channel coefficients

for each antenna block. This application leads the system to select the antenna blocks and antennas in each block, not only by the BNM Bits and ANM Bits, but also the channel amplitude responses of each block and antenna that blocks contain. Multiple Multiple Input Multiple Output System with Antenna Number Modulation and Adaptive Antenna Selection (M-MIMO-ANM-AAS) is designed to select the best antennas among the best antenna blocks.

The application procedure of M-MIMO-ANM-AAS is explained as follows:

1) By sending an experimental signal from the receiver in a Time Division Duplex (TDD) system, the transmitter estimates the channel amplitude responses of each transmit antenna.
2) As the next step, the average values of each adjacent T antennas in one block are calculated to assign a channel amplitude value to each antenna block.
3) Within this step, the transmitter can achieve the detection of the channel amplitude values of antenna blocks with respect to the receiver. For a singular receive antenna at the reception end and B antenna blocks at the transmission end, the channel amplitude vector of antenna blocks becomes $|\mathbf{g}| = [|g_{11}|, |g_{12}|, |g_{13}|, ..., |g_{1B}|] \in \mathbb{C}^{1\times B}$.
4) The channel response values of vector $|\mathbf{g}|$ is then sorted by the transmitter from its highest value to lowest value.
5) After the ranking of the blocks is done, the channel amplitude values of transmit antennas, which are previously obtained for the detection of the channel amplitude values of antenna blocks, are specified for each block that contains T transmit antennas. For a singular receive antenna at the reception and T transmit antennas in each of B blocks the channel amplitude vector of transmit antennas becomes $|\mathbf{h}| = [|h_{11}|, |h_{12}|, |h_{13}|, ..., |h_{1T_{Total}}|] \in \mathbb{C}^{1\times T_{Total}}$.
6) For the next step, the transmitter maximizes the SNR of the receiver, which leads to an increase in the reliability performance of the receiver since it reduces the BER of the system. Even though, there are many strategies[3] to select antennas according to their channel gains, in this study transmitter deploys the strategy that suggests using the antennas that provides the largest channel gain, thanks to block and antenna number selective nature of number modulation scheme rather than their indices or positions in the system.
7) The selection process in M-MIMO-ANM-AAS, which comes after the decision that how many antenna blocks and transmit antennas in each block are activated by BNM Bits and ANM Bits respectively, relies on activating specific antenna blocks and specific transmit antennas in those certain amounts of antenna blocks and transmit antennas that are specified by BNM Bits and ANM Bits, according to their channel coefficient qualities.

By the given equation below, the optimal antenna block selection positions of the antenna blocks can be calculated according to their SNR values

$$\{\zeta_1^{opt}, \cdots, \zeta_Z^{opt}\} = \arg \max_{\{\zeta_1,\cdots,\zeta_Z\}\in\mathcal{A}_Z} SNR_{[\zeta_1,\cdots,\zeta_Z]}, \tag{22}$$

where $\mathcal{A}_Z$ is the possible combinations of antenna block activation patterns, $SNR_{[\zeta_1,\cdots,\zeta_Z]}$ is the summation of the SNR values that is acquired from Z number of activated antenna blocks in the system.

A similar equation is given below to calculate the optimal antenna selection positions of the transmit antennas in each active block according to their SNR values

$$\{v_1^{opt}, \cdots, v_V^{opt}\} = \arg \max_{\{v_1,\cdots,v_V\}\in\mathcal{A}_V} SNR_{[v_1,\cdots,v_V]}, \tag{23}$$

where $\mathcal{A}_V$ is the possible combinations of transmit antenna activation patterns in each activated antenna block, $SNR_{[v_1,\cdots,v_V]}$ is the summation of the SNR values of that is acquired from V number of activated transmit antennas in each antenna block.

In order to take these equations one step further, antenna block selection and transmit antenna selection in each block can be achieved by the channel coefficients, since a uniform power allocation is used in the system. The corresponding equations for antenna block selection and transmit antenna selection in each block are given below

$$\{\zeta_1^{opt}, \cdots, \zeta_Z^{opt}\} = \arg \max_{\{\zeta_1,\cdots,\zeta_Z\}\in\mathcal{A}_Z} |g_{1Z}|_{[\zeta_1,\cdots,\zeta_Z]}, \tag{24}$$

$$\{v_1^{opt}, \cdots, v_V^{opt}\} = \arg \max_{\{v_1,\cdots,v_V\}\in\mathcal{A}_V} |h_{1V}|_{[v_1,\cdots,v_V]}, \tag{25}$$

Example: Another example that deeply explains the M-MIMO-ANM scheme is given as follows. However, in this example, the Adaptive Antenna Selection feature of the system is emphasized. Assume the same sample of data sequence that is used in the first example as given in Fig. 2, and this data sequence is desired to be sent by the same amount of antenna blocks, same amount of transmit antennas, and the same amount of receive antennas as the first example (ie., $B\times T\times R = 4\times4\times1$ or $T_{Total}\times R = 16\times1$) in an M-MIMO-ANM-AAS system. Let the coefficients of the transmission part of the system is notified as in Fig. 5.

In this figure, the first column demonstrates the illustrations of the antenna blocks, transmit antennas, and

[3]It should be stated that there are many strategies in the literature to achieve the antenna selection in MIMO systems, such as Euclidean distance-based or capacity-based transmit antenna selection schemes, which is used in literature [29]–[33] for MIMO-SM. However, by doing the selection of antenna blocks and transmit antennas in each block according to the largest channel gains, leads to the system to be much simpler, more cost effective and less complex in M-MIMO-ANM case.

Base Station Blocks	Antennas	Antenna Coefficients (h)	Absolute Values of Antenna Coefficients (|h|)	Block Coefficients (g)	Absolute Values of Block Coefficients (|g|)
B_1	Tx_1	$h_{1/1}$=0.7782-0.1386i	$\|h_{1/1}\|$=0.7905	$g_{1/1}=(h_{1/1}+h_{1/2}+h_{1/3}+h_{1/4})/4$ =0.8762+1.2111i	$\|g_{1/1}\|$=1.4948
	Tx_2	$h_{1/2}$=1.0919+1.0036i	$\|h_{1/2}\|$=1.4831		
	Tx_3	$h_{1/3}$=0.0608+0.2062i	$\|h_{1/3}\|$=0.2149		
	Tx_4	$h_{1/4}$=-1.0547+0.1399i	$\|h_{1/4}\|$=1.0639		
B_2	Tx_5	$h_{1/5}$=-0.5249+1.1227i	$\|h_{1/5}\|$=1.2393	$g_{1/2}=(h_{1/5}+h_{1/6}+h_{1/7}+h_{1/8})/4$ =-0.0489+1.6370i	$\|g_{1/2}\|$=1.6377
	Tx_6	$h_{1/6}$=-0.7507-0.5688i	$\|h_{1/6}\|$=0.9418		
	Tx_7	$h_{1/7}$=1.6620+0.4926i	$\|h_{1/7}\|$=1.7335		
	Tx_8	$h_{1/8}$=-0.4353+0.5905i	$\|h_{1/8}\|$=0.7336		
B_3	Tx_9	$h_{1/9}$=0.5290-0.1723i	$\|h_{1/9}\|$=0.5563	$g_{1/3}=(h_{1/9}+h_{1/10}+h_{1/11}+h_{1/12})/4$ =0.4804-1.6559i	$\|g_{1/3}\|$=1.7242
	Tx_{10}	$h_{1/10}$=-0.1361+0.1525i	$\|h_{1/10}\|$=0.2044		
	Tx_{11}	$h_{1/11}$=0.6283-0.8244i	$\|h_{1/11}\|$=1.0365		
	Tx_{12}	$h_{1/12}$=-0.5408-0.8117i	$\|h_{1/12}\|$=0.9754		
B_4	Tx_{13}	$h_{1/13}$=-0.9916+0.0742i	$\|h_{1/13}\|$=0.9943	$g_{1/4}=(h_{1/13}+h_{1/14}+h_{1/15}+h_{1/16})/4$ =-1.7776+1.9415i	$\|g_{1/4}\|$=2.6324
	Tx_{14}	$h_{1/14}$=-1.0058+0.5107i	$\|h_{1/14}\|$=1.1280		
	Tx_{15}	$h_{1/15}$=0.3452+1.8282i	$\|h_{1/15}\|$=1.8605		
	Tx_{16}	$h_{1/16}$=-0.1254-0.4716i	$\|h_{1/16}\|$=0.4880		

FIGURE 5: Variable Table of the Given Example.

their notations as B_1, B_2, B_3, B_4 for transmit antenna blocks, and from T_1 through T_{16} for transmit antennas. The second, "Antenna Coefficients", column that is notated as h is the flat fading channel coefficients for each individual antenna element. In the third, "Absolute Values of Antenna Coefficients", column the absolute values of each complex number are calculated to be able to make a proper sorting among antennas in each block under the notation of $|h|$. The variable notated as g in the forth, "Block Coefficients", column is the average values of each four adjacent antennas, which defines the flat fading channel coefficients for each block. To take the quality ranking in the block level, each value that are calculated in Block Coefficients column are considered as their absolute values in fifth, "Absolute Values of Block Coefficients", column which is notated as $|g|$.

According to this table by examining the *Absolute Values of Block Coefficients* column, it can be obviously detected that the quality ranking of each transmit

TABLE 3: The calculated statistics of the effective Rayleigh fading channel amplitude of MISO-ANM with B=4, T=4

BNM Bits (ζ)	ANM Bits ($\mathbf{v}$)	Active Antennas Pattern	$\lvert h_{eff}\rvert$	Scale (β)	Mean Square ($\overline{\alpha^2}$)
[0 0]	[0 0]	[1 0 0 0 0 0 0 0 0 0 0 0 0 0 0 0]	$\lvert g_1 \times h_1\rvert$	0.681	1
[0 0]	[0 1]	[1 1 0 0 0 0 0 0 0 0 0 0 0 0 0 0]	$\lvert g_1 \times (h_1 + h_2)\rvert$	1.371	2
[0 0]	[1 0]	[1 1 1 0 0 0 0 0 0 0 0 0 0 0 0 0]	$\lvert g_1 \times (h_1 + h_2 + h_3)\rvert$	2.013	3
[0 0]	[1 1]	[1 1 1 1 0 0 0 0 0 0 0 0 0 0 0 0]	$\lvert g_1 \times (h_1 + h_2 + h_3 + h_4)\rvert$	2.726	4
[0 1]	[0 0]	[1 0 0 0 1 0 0 0 0 0 0 0 0 0 0 0]	$\lvert g_1 \times (h_1) + g_2 \times (h_5)\rvert$	1.371	2
[0 1]	[0 1]	[1 1 0 0 1 1 0 0 0 0 0 0 0 0 0 0]	$\lvert g_1 \times (h_1 + h_2) + g_2 \times (h_5 + h_6)\rvert$	2.726	4
[0 1]	[1 0]	[1 1 1 0 1 1 1 0 0 0 0 0 0 0 0 0]	$\lvert g_1 \times (h_1 + h_2 + h_3) + g_2 \times (h_5 + h_6 + h_7)\rvert$	4.027	6
[0 1]	[1 1]	[1 1 1 1 1 1 1 1 0 0 0 0 0 0 0 0]	$\lvert g_1 \times (h_1 + h_2 + h_3 + h_4) + g_2 \times (h_5 + h_6 + h_7 + h_8)\rvert$	5.467	8
[1 0]	[0 0]	[1 0 0 0 1 0 0 0 1 0 0 0 0 0 0 0]	$\lvert g_1 \times (h_1) + g_2 \times (h_5) + g_3 \times (h_9)\rvert$	2.013	3
[1 0]	[0 1]	[1 1 0 0 1 1 0 0 1 1 0 0 0 0 0 0]	$\lvert g_1 \times (h_1 + h_2) + g_2 \times (h_5 + h_6) + g_3 \times (h_9 + h_{10})\rvert$	4.027	6
[1 0]	[1 0]	[1 1 1 0 1 1 1 0 1 1 1 0 0 0 0 0]	$\lvert g_1 \times (h_1 + h_2 + h_3) + g_2 \times (h_5 + h_6 + h_7) + g_3 \times (h_9 + h_{10} + h_{11})\rvert$	6.155	9
[1 0]	[1 1]	[1 1 1 1 1 1 1 1 1 1 1 1 0 0 0 0]	$\lvert g_1 \times (h_1 + h_2 + h_3 + h_4) + g_2 \times (h_5 + h_6 + h_7 + h_8) + g_3 \times (h_9 + h_{10} + h_{11} + h_{12})\rvert$	8.275	12
[1 1]	[0 0]	[1 0 0 0 1 0 0 0 1 0 0 0 1 0 0 0]	$\lvert g_1 \times (h_1) + g_2 \times (h_5) + g_3 \times (h_9) + g_4 \times (h_{13})\rvert$	2.726	4
[1 1]	[0 1]	[1 1 0 0 1 1 0 0 1 1 0 0 1 1 0 0]	$\lvert g_1 \times (h_1 + h_2) + g_2 \times (h_5 + h_6) + g_3 \times (h_9 + h_{10}) + g_4 \times (h_{13} + h_{14})\rvert$	5.467	8
[1 1]	[1 0]	[1 1 1 0 1 1 1 0 1 1 1 0 1 1 1 0]	$\lvert g_1 \times (h_1 + h_2 + h_3) + g_2 \times (h_5 + h_6 + h_7) + g_3 \times (h_9 + h_{10} + h_{11}) + g_4 \times (h_{13} + h_{14} + h_{15})\rvert$	8.275	12
[1 1]	[1 1]	[1 1 1 1 1 1 1 1 1 1 1 1 1 1 1 1]	$\lvert g_1 \times (h_1 + h_2 + h_3 + h_4) + g_2 \times (h_5 + h_6 + h_7 + h_8) + g_3 \times (h_9 + h_{10} + h_{11} + h_{12}) + g_4 \times (h_{13} + h_{14} + h_{15} + h_{16})\rvert$	10.910	16

antenna block is ordered as $|g_{1/4}|) > |g_{1/3}| > |g_{1/2}| > |g_{1/1}|$, which means that the first priority of the block selection belongs to B_4, then B_3, then B_2, then B_1. By analysing the antenna qualities in each block, it can be seen that the quantities of the $|h|$ values are ordered as $|h_{1/2}| > |h_{1/4}| > |h_{1/1}| > |h_{1/3}|$ in the B_1, which means T_2 offers the best channel quality, T_4 offers the second and T_1 offers the third best channel qualities, whereas T_3 offers the worst channel quality in B_1. Similarly, the channel quality orders, which also defines the antenna activation priority patterns of each transmit antenna in each antenna block can be specified from highest to lowest as T_7, T_5, T_6, T_8 for B_2, $T_{11}, T_{12}, T_9, T_{10}$ for B_3, and $T_{15}, T_{12}, T_{13}, T_{16}$ for B_4.

Within this knowledge, the given data stream 101101101011011 is separated as Main Bits, BNM Bits, and ANM Bits to start the M-MIMO-ANM process. Transmission of the first bit in the Main Bits group, 1, three blocks that provide the best channel qualities are deployed, since the corresponding block number is 10. In these best quality offering blocks, two highest channel quality offering antennas are activated, since the first two bits in the ANM Bits group is 01.

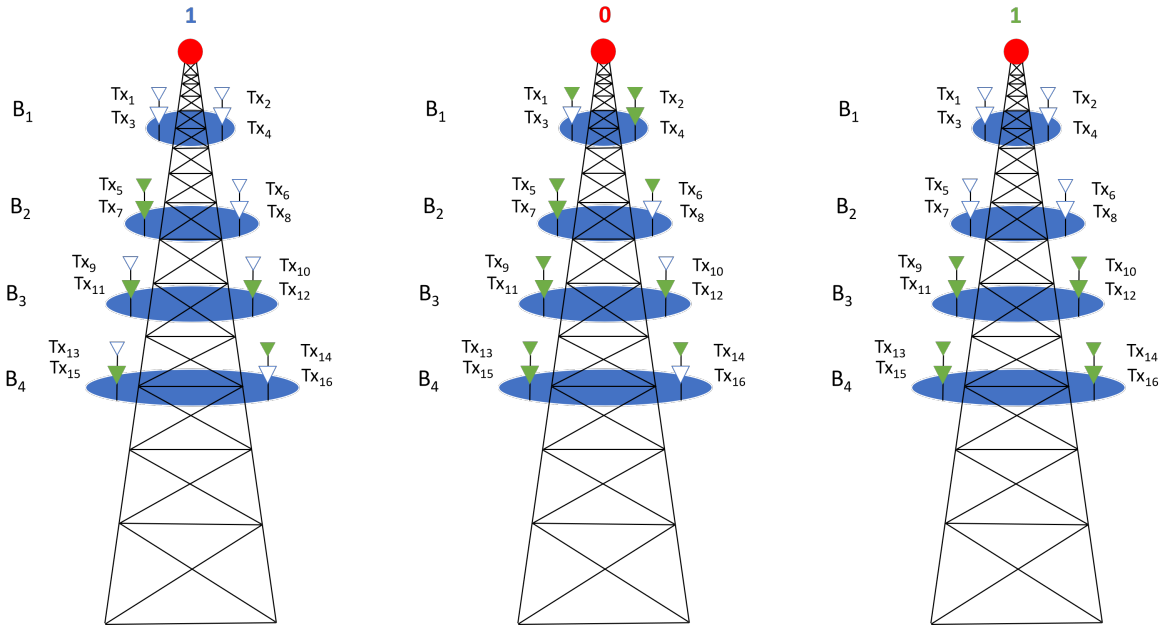

((**a**)) Transmission of 1 via three blocks two antennas in each block.

((**b**)) Transmission of 0 via four blocks three antennas in each block.

((**c**)) Transmission of 1 via two blocks four antennas in each block.

FIGURE 6: Simple visualization of the antenna activation process and mapping in M-MIMO-ANM-AAS scheme.

Thus, the transmission of the first element of the Main Bits group, 1, is operated by T_{15}, T_{14} as the member of B_4, which is the highest channel quality offering antenna block, T_{11}, T_{12} as the member of B_3, which is the second highest channel quality offering antenna block, and T_7, T_5 as the member of B_2, which is the third highest channel quality offering antenna block. The second bit in the Main Bits group 0, is sent by four blocks, since the second couple of bits in BNM Bits group is 11, which means the channel qualities of antenna blocks, in this case, do not matter since the all blocks are activated. However, the antenna qualities in each active block still must be taken into consideration. The second couple, 01, in ANM Bits group is assigned, in order to decide which transmit antennas are opened in each antenna block, which indicates the activation of two transmit antennas for B_1, B_2, B_3, B_4 separately. According to Fig. 5, the highest channel quality offering antennas are T_{15}, T_{14}, T_{13} for B_4 as the first prioritized antenna block, T_{11}, T_{12}, T_9 for B_3 as the second prioritized antenna block, T_7, T_5, T_6 for B_2 as the third prioritized antenna block, and T_2, T_4, T_1 for B_2 as the forth prioritized antenna block. Since the last couples of BNM Bits and ANM Bits groups are 01, and 11 respectfully, the last bit in the Main Bits group, 0, is meant to be sent via two antenna blocks that provide the most qualified conditions with their all containing antennas. As previously stressed, the two most channel ranked blocks are B_4, and B_3 in descending order. Thus, the transmission of 0 is operated by all the containing antennas of these two blocks. All these processes are illustrated in Fig. 6.

IV. PERFORMANCE ANALYSIS OF M-MIMO-ANM

A. STATISTICS OF THE EFFECTIVE INSTANTANEOUS SNR

Because of the fact that for different number of active antenna blocks and transmit antennas in these blocks for different activation patterns, the original fading distribution parameters are not appropriate for the proposed M-MIMO-ANM. The reason why the original fading distribution channel is not appropriate for the M-MIMO-ANM can be explained by considering the data transmission process. In M-MIMO-ANM, at each channel use the antenna numbers and indices change according to BNM and ANM bits, which means the transmission slots are not always stable. That's why the fading distribution parameters are always reconfigured by the active antenna blocks and active transmit antennas in these active blocks. This reconfiguration of fading distribution parameters is achieved by obtaining the amplitude and power of each fading channel. To obtain these parameters, a method so called numerical data fitting is used, which is explained in detail in [26].

In M-MIMO-ANM scheme, the active antenna patterns are decided by BNM bits and ANM bits, which may exhibit a random variety for the number of antenna blocks and antennas in each active block for the data transmission. Therefore, an intuitive approach is adopted to obtain a similar distribution to the original fading distribution. Acquired results prove that the intuitive distribution results from the

simulations, which are named as the effective distribution, show very similar characteristics to the Rayleigh distribution with different scale factors and means, as shown in Table 3. The following formula represents the amplitude channel distribution.

$$f_\alpha(\alpha) = \frac{\alpha}{\beta^2}\exp\left(-\frac{\alpha^2}{2\beta^2}\right), \tag{26}$$

where β is th scale parameter and $\alpha = h_{eff}$ is the Rayleigh channel distribution amplitude, $\omega = \alpha^2$ is represented as the mean square of α, which is also equal to ψ where ψ is the mean factor as a vital parameter in the channel power calculation of the effective channel. These distribution parameters are given in Table 3 for the proposed M-MIMO-ANM.

In order to generate a power distribution function (PDF) for the $\gamma = \frac{|h_{eff}|^2 P}{\sigma^2}$, following expression is given as

$$f_\gamma(\gamma) = \frac{f_\alpha\left(\sqrt{\frac{\Omega\gamma}{\bar{\gamma}}}\right)}{\frac{1}{\beta^2}\sqrt{\frac{\bar{\gamma}\gamma}{\Omega}}} \tag{27}$$

By using these calculated distribution functions above, BER performance of the proposed M-MIMO-ANM can be analyzed properly.

B. ERROR PERFORMANCE ANALYSIS OF M-MIMO-ANM

In the proposed M-MIMO-ANM scheme, there are three stages that operate the estimation. The first one is the estimation of the number of antenna blocks, second is the estimation of number of transmit antennas, and the third one is the transmission of estimated bits, which makes the analytical performance analysis more complicated. However, the following derived equation offers a correct performance analysis.

Let the three stages of the estimation process is notated by A_1, A_2, and A_3 for the number of blocks estimation, the number of antenna estimation, and transmitted bit estimation, respectively. Even though the data stream grouping is the same for the BNM bits and ANM bits, it is not the same for the Main Bits. There are two bits used in each BNM and ANM bits groups for the transmission of one bit in the Main Bits group. Therefore, their respective probabilities are $P(A_1) = 2/5$, $P(A_2) = 2/5$, $P(A_3) = 1/5$. By assuming the $P_{BNM}(E)$ and $P_{ANM}(E)$ are the error probabilities for A_1 and A_2, respectively. $P_{BPSK}(E)$ is the error probability for Main bits which is modulated by BPSK, the total error probability $P_{Total}(E)$ can be formulated as

$$\begin{aligned} P_{tot}(E) = {} & P_{BNM}(E|A_1)P(A_1) + P_{ANM}(E|A_2)P(A_2) \\ & + P_{BPSK}(E|A_3)P(A_3) \end{aligned} \tag{28}$$

$$P_{tot}(E) = \frac{2}{5}P_{BNM}(E) + \frac{2}{5}P_{ANM}(E) + \frac{1}{5}P_{BPSK}(E) \tag{29}$$

V. AVERAGE BER PERFORMANCE OF ALL POSSIBLE ANTENNA NUMBER ACTIVATION PATTERNS

In this section, possible error calculations are represented in terms of three parameters; error caused by the BNM bits detection, error caused by the ANM bits detection, and error caused by the Main Bits detection.

As the first reason of error, the general BER formula of BNM Bits are given as follows:

$$BER_{BNM-i} = \frac{2}{T_{Total}} \times \left(1 - \sqrt{\frac{\frac{\sqrt{\theta_i}\times E_b}{3\times B_{act}\times N_0}}{\frac{\sqrt{\theta_i}\times E_b}{3\times B_{act}\times N_0}+1}}\right) \tag{30}$$

where; i is the iterator from 1 to B,
T_{Total} is the total number of transmit antennas in the system,
β is the scale factor for the antenna activation pattern, and
θ is the summation of the scale factors of the antennas in the antenna blocks.
B_{act} is the number of active antenna blocks among the whole antenna blocks.

After the BER results are calculated for each antenna block activation case, the average value of these results determines the BER performance of BNM bits as shown below.

$$BER_{BNM} = \frac{\sum_{i=1}^{B} BER_{BNM-i}}{B}. \tag{31}$$

As the second reason of error, the general BER formula of ANM Bits are given as follows:

$$BER_{ANM-i} = \frac{2}{T_{Total}} \times \left(1 - \sqrt{\frac{\frac{B_{act}\times T_{act}\times E_b}{2\times\sqrt{\beta_i}\times N_0}}{\frac{B_{act}\times T_{act}\times E_b}{2\times\sqrt{\beta_i}\times N_0}+1}}\right) \tag{32}$$

where; i is the iterator from 1 to T_{Total},
T_{act} is the number of active transmit antennas in the active antenna blocks.

After the BER results are calculated for each antenna block and transmit antenna activation case, the average value of these results determine the BER performance of ANM bits as shown below.

$$BER_{ANM} = \frac{\sum_{i=1}^{T_{Total}} BER_{ANM-i}}{T_{Total}}. \tag{33}$$

As the third reason of error, the general BER formula of ANM Bits are given as follows:

$$BER_{Main-i,j} = 0.4\times \left(1 - \sqrt{\frac{\frac{2\times\theta_i\times\beta_j\times E_b}{B_{act}\times T_{act}\times N_0}}{\frac{2\times\theta_i\times\beta_j\times E_b}{B_{act}\times T_{act}\times N_0}+1}}\right) \tag{34}$$

where; i is the iterator from 1 to B,
j is the iterator from 1 to T_{Total}, which for each four iteration of j, i iterates one,

After the BER results are calculated for each antenna block activation case, the average value of these results determines the BER performance of Main bits as shown below.

$$BER_{Main} = \frac{\sum_{i,j=1}^{B,T_{Total}} BER_{Main-i,j}}{16}. \quad (35)$$

As a result of these BER calculations of BNM bits, ANM bits, and Main Bits the average BER of the M-MIMO-ANM system for BPSK is calculated as

$$BER_{M-MIMO-ANM} = \frac{2}{5} \times BER_{BNM} + \frac{2}{5} \times BER_{ANM} + \frac{1}{5} \times BER_{Main}. \quad (36)$$

VI. PERFORMANCE DEMONSTRATION

Within this section, by running the Monte-Carlo simulations for each offered scheme, Multiple MIMO-ANM, and Multiple MIMO-ANM-AAS, the performance results of each scheme are exhibited over a Rayleigh fading channel in terms of BER. In the conduction of the system number of antenna blocks and number of transmit antennas in each block are considered to be four $(B = 4, T = 4)$, which means the total number of transmit antennas in the whole system is sixteen $(T_{Total} = 16)$, whereas the number of antennas at the reception side of the system is assumed to be one $(R = 1)$.

Even though a comparison of a less amount of transmit antenna containing Multiple MIMO-ANM scheme with the conventional MIMO-ANM scheme, which contains only four transmit antennas, would provide a better understanding in terms of the superiority of Multiple MIMO-ANM system, it would require to keep either one of those transmission antenna blocks or transmit antennas in each block singular to acquire four transmit antennas at the transmission end, which makes the purpose of the proposed Multiple MIMO-ANM scheme meaningless. Regarding this problem, Monte-Carlo simulations of the conventional MIMO-ANM are reconducted for this study, and the number of transmit antennas is changed to sixteen, to properly see the contribution of a block number sensitive transmission algorithm on the MIMO-ANM system. The parameters used in the simulations for different varieties of modulation types are given in Table 4.

TABLE 4: Simulation Parameters

Modulation Type	BPSK (M=2)
Number of Symbols	10^6 per iteration
Number of Antenna Blocks	4
Number of Transmit Antennas	4
Number of Receive Antennas	1
Number of available antennas for ANM	16
Number of BNM mapping bits	2
Number of ANM mapping bits	2
Wireless channel	Block Rayleigh fading

Fig. 7 shows the numerically analyzed BER performance of the proposed M-MIMO-ANM and M-MIMO-ANM-AAS. Fig. 7 also shows the comparison of M-MIMO-ANM and conventional MIMO-ANM under different number of transmit antenna conditions (i.e. $T = 4$, $T = 16$). As the Fig. 7 indicates, even the transmit antenna number is increased to sixteen in conventional MIMO-ANM to equalize the transmit antenna number with M-MIMO-ANM, the effect of the transmit antenna blocks creates an advantage for M-MIMO-ANM, even both conventional MIMO-ANM and proposed M-MIMO-ANM are considered under the same antenna number conditions. This significant gain results in a higher data coverage rate and more effective transmit power management without sacrificing any requirements of the service operations.

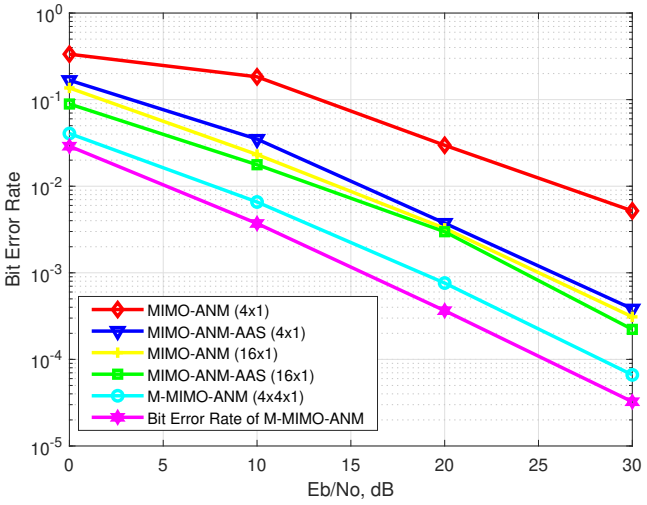

FIGURE 7: Comparison of Different ANM Schemes Under BPSK Conditions.

Fig. 8 illustrates the average error rates of each bit group in the given data stream, namely, BNM bits, which are modulated by the number of antenna blocks, ANM bits, which are modulated by the number of transmit antennas in each block, and Main bits, which are modulated by BPSK. From this figure, it can be observed that as the SNR value is increased from 0 to 30, the BER performances of each bit group is getting better results, as compared with conventional MIMO-ANM.

Since both M-MIMO-ANM and conventional MIMO-ANM schemes are capable of transmission five bits at a time in a sixteen transmit antenna case, it might be considered why the M-MIMO-ANM is more preferable than conventional MIMO-ANM. To explain this, several reasons can be offered. The first reason is obviously the superior performance of M-MIMO-ANM, that is caused by the extra channel boost by the antenna blocks as shown in Fig. 7 . The second reason is the lower complexity that the M-MIMO-ANM offers. By dividing the ANM bits in conventional MIMO-ANM as BNM bits and ANM bits for M-MIMO-ANM results in

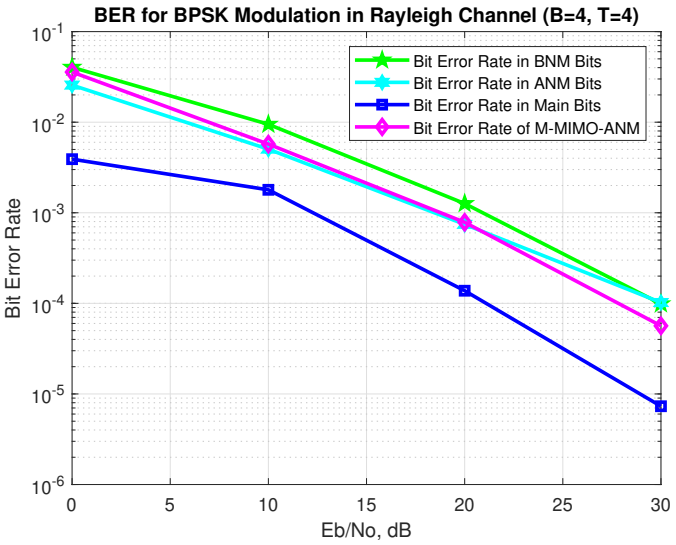

FIGURE 8: Simulation Results of Multiple MIMO-ANM Under BPSK Modulation Conditions.

activating less number of antennas without sacrificing from BER performance.

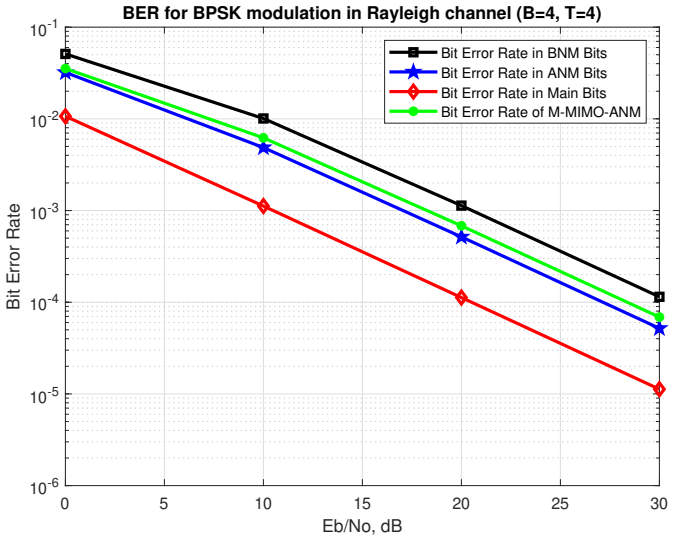

FIGURE 9: Theoretical Calculation Results of Multiple MIMO-ANM Under BPSK Modulation Conditions.

Lastly, Fig. 9 is the exhibition of the derived BER formulas for M-MIMO-ANM, where the overall average theoretical BER performance indicated in green color curve shows similar characteristics with the simulated BER performance that is shown in Fig. 8.

VII. CONCLUSION

In this paper, M-MIMO-ANM scheme is proposed as a new data transmission method. The basic idea behind M-MIMO-ANM is increasing the number of transmit antennas and locating them into groups, namely the antenna blocks. By doing this, M-MIMO-ANM creates an opportunity to deploy a new dimension which is the number of antenna blocks, in addition to the number of antennas to convey extra data bits beside the transmitted bits by the antenna number modulation and conventional M-ary PSK/QAM symbols. The advantages of the M-MIMO-ANM over conventional MIMO-ANM is the lower BER performance and higher data rate in addition to the lower complexity and ability to make not only the best antenna selection, but also the best antenna block selection that is created by the best antennas.

REFERENCES

[1] Erik G Larsson, Ove Edfors, Fredrik Tufvesson, and Thomas L Marzetta. Massive mimo for next generation wireless systems. IEEE communications magazine, 52(2):186–195, 2014.

[2] Jakob Hoydis, Cornelis Hoek, Thorsten Wild, and Stephan ten Brink. Channel measurements for large antenna arrays. In 2012 International Symposium on Wireless Communication Systems (ISWCS), pages 811–815. IEEE, 2012.

[3] T Lakshmi Narasimhan, Patchava Raviteja, and A Chockalingam. Generalized spatial modulation in large-scale multiuser mimo systems. IEEE Transactions on Wireless Communications, 14(7):3764–3779, 2015.

[4] Jehad M Hamamreh, Abdulwahab Hajar, and Mohamedou Abewa. Orthogonal frequency division multiplexing with subcarrier power modulation for doubling the spectral efficiency of 6g and beyond networks. Transactions on Emerging Telecommunications Technologies, 31(4):e3921, 2020.

[5] Fredrik Rusek, Daniel Persson, Buon Kiong Lau, Erik G Larsson, Thomas L Marzetta, Ove Edfors, and Fredrik Tufvesson. Scaling up mimo: Opportunities and challenges with very large arrays. IEEE signal processing magazine, 30(1):40–60, 2012.

[6] Lu Lu, Geoffrey Ye Li, A Lee Swindlehurst, Alexei Ashikhmin, and Rui Zhang. An overview of massive mimo: Benefits and challenges. IEEE journal of selected topics in signal processing, 8(5):742–758, 2014.

[7] Linglong Dai, Zhaocheng Wang, and Zhixing Yang. Spectrally efficient time-frequency training ofdm for mobile large-scale mimo systems. IEEE Journal on Selected Areas in Communications, 31(2):251–263, 2013.

[8] Thomas L Marzetta. Noncooperative cellular wireless with unlimited numbers of base station antennas. IEEE transactions on wireless communications, 9(11):3590–3600, 2010.

[9] Long Zhao, Kan Zheng, Hang Long, and Hui Zhao. Performance analysis for downlink massive mimo system with zf precoding. Transactions on Emerging Telecommunications Technologies, 25(12):1219–1230, 2014.

[10] Emil Björnson, Jakob Hoydis, Marios Kountouris, and Merouane Debbah. Massive mimo systems with non-ideal hardware: Energy efficiency, estimation, and capacity limits. IEEE Transactions on Information Theory, 60(11):7112–7139, 2014.

[11] Yuanyuan Hao, Zhengyu Song, Shujuan Hou, and Hai Li. Energy- and spectral-efficiency tradeoff in massive mimo systems with inter-user interference. In 2015 IEEE 26th Annual International Symposium on Personal, Indoor, and Mobile Radio Communications (PIMRC), pages 553–557. IEEE, 2015.

[12] Chao-Kai Wen, Wan-Ting Shih, and Shi Jin. Deep learning for massive mimo csi feedback. IEEE Wireless Communications Letters, 7(5):748–751, 2018.

[13] Yong Zeng, Rui Zhang, and Zhi Ning Chen. Electromagnetic lens-focusing antenna enabled massive mimo: Performance improvement and cost reduction. IEEE Journal on Selected Areas in Communications, 32(6):1194–1206, 2014.

[14] Le Liang, Wei Xu, and Xiaodai Dong. Low-complexity hybrid precoding in massive multiuser mimo systems. IEEE Wireless Communications Letters, 3(6):653–656, 2014.

[15] Sohail Payami and Fredrik Tufvesson. Channel measurements and analysis for very large array systems at 2.6 ghz. In 2012 6th European Conference on Antennas and Propagation (EUCAP), pages 433–437. IEEE, 2012.

[16] Ke Xu, Hongyi Yu, and Yi-Jun Zhu. Channel-adapted spatial modulation for massive mimo visible light communications. IEEE Photonics Technology Letters, 28(23):2693–2696, 2016.

[17] Yuan Gao, Wei Jiang, and Thomas Kaiser. Bidirectional branch and bound based antenna selection in massive mimo systems. In 2015 IEEE 26th Annual International Symposium on Personal, Indoor, and Mobile Radio Communications (PIMRC), pages 563–568. IEEE, 2015.
[18] Xiang Gao, Ove Edfors, Jianan Liu, and Fredrik Tufvesson. Antenna selection in measured massive mimo channels using convex optimization. In 2013 IEEE globecom workshops (GC Wkshps), pages 129–134. IEEE, 2013.
[19] Bing Fang, Zuping Qian, Wei Shao, and Wei Zhong. Raise: A new fast transmit antenna selection algorithm for massive mimo systems. Wireless personal communications, 80(3):1147–1157, 2015.
[20] Ke Dong, Narayan Prasad, Xiaodong Wang, and Shihua Zhu. Adaptive antenna selection and tx/rx beamforming for large-scale mimo systems in 60 ghz channels. EURASIP Journal on Wireless Communications and Networking, 2011(1):59, 2011.
[21] Maria Gkizeli and George N Karystinos. Maximum-snr antenna selection among a large number of transmit antennas. IEEE Journal of Selected Topics in Signal Processing, 8(5):891–901, 2014.
[22] Dushyantha A Basnayaka, Marco Di Renzo, and Harald Haas. Massive but few active mimo. IEEE Transactions on Vehicular Technology, 65(9):6861–6877, 2015.
[23] Ahmad M Jaradat, Jehad M Hamamreh, and Huseyin Arslan. Ofdm with subcarrier number modulation. IEEE Wireless Communications Letters, 7(6):914–917, 2018.
[24] Ahmad M Jaradat, Jehad M Hamamreh, and Hüseyin Arslan. Modulation options for ofdm-based waveforms: classification, comparison, and future directions. IEEE Access, 7:17263–17278, 2019.
[25] Ahmad M Jaradat, Jehad M Hamamreh, and Hüseyin Arslan. Ofdm with hybrid number and index modulation. IEEE Access, 8:55042–55053, 2020.
[26] Jehad M. Hamamreh, MUHAMMET KIRIK, MEHMET O. SAGMAN, and NAOKI ISHIKAWA. Multiple input multiple output with antenna number modulation and adaptive antenna selection. RS Open Journal on Innovative Communication Technologies, 6 2020. https://rs-ojict.pubpub.org/pub/mimo-anm.
[27] Miaowen Wen, Qiang Li, Ertugrul Basar, and Wensong Zhang. Generalized multiple-mode ofdm with index modulation. IEEE Transactions on Wireless Communications, 17(10):6531–6543, 2018.
[28] Miaowen Wen, Beixiong Zheng, Kyeong Jin Kim, Marco Di Renzo, Theodoros A Tsiftsis, Kwang-Cheng Chen, and Naofal Al-Dhahir. A survey on spatial modulation in emerging wireless systems: Research progresses and applications. IEEE Journal on Selected Areas in Communications, 37(9):1949–1972, 2019.
[29] Ping Yang, Yue Xiao, Lei Li, Qian Tang, Yi Yu, and Shaoqian Li. Link adaptation for spatial modulation with limited feedback. IEEE Transactions on Vehicular Technology, 61(8):3808–3813, 2012.
[30] Rakshith Rajashekar, KVS Hari, and Lajos Hanzo. Antenna selection in spatial modulation systems. IEEE Communications Letters, 17(3):521–524, 2013.
[31] Konstantinos Ntontin, Marco Di Renzo, Ana I Pérez-Neira, and Christos Verikoukis. A low-complexity method for antenna selection in spatial modulation systems. IEEE communications letters, 17(12):2312–2315, 2013.
[32] Yuanyuan He, Saman Atapattu, Chintha Tellambura, and Jamie S Evans. Opportunistic group antenna selection in spatial modulation systems. IEEE Transactions on Communications, 66(11):5317–5331, 2018.
[33] Rakshith Rajashekar, Lie-Liang Yang, KVS Hari, and Lajos Hanzo. Transmit antenna subset selection in generalized spatial modulation systems. IEEE Transactions on Vehicular Technology, 68(2):1979–1983, 2018.

MUHAMMET KIRIK He is a senior electrical and electronics engineering student at Antalya International (Bilim) University, Turkey. His current research interests include orthogonal frequency-division multiplexing multiple-input multiple-output systems, multi-dimensional modulation techniques, and orthogonal/non-orthogonal multiple access schemes for future wireless systems.

JEHAD M. HAMAMREH is currently an Assistant Professor with the Electrical and Electronics Engineering Department, Antalya International (Bilim) University, Turkey. He received the Ph.D. degree in electrical-electronics engineering and Cyber systems from Istanbul Medipol University, Turkey, in 2018. He worked as a Researcher at the Department of Electrical and Computer Engineering in Texas AM University. He is the inventor of 8+ Patents, and He has authored more than 55+ peer reviewed scientific papers along with several book chapters. His innovative patented works won the golden, silver and bronze medals by numerous international invention contests and fairs. His current research interests include wireless physical and MAC layers security, orthogonal frequency-division multiplexing multiple-input multiple-output systems, advanced waveforms design, multidimensional modulation techniques, and orthogonal/non-orthogonal multiple access schemes for future wireless systems. He is a regular investigator and referee for various scientific journals as well as a TPC member for several international conferences. He is an Editor at RS-OJICT and Frontiers in Communications and Networks. He can be reached at jehad.hamamreh@gmail.com.